

RESEARCH ARTICLE

Changes in absolute gravity 2000–2015, South Island, New Zealand

Roger Bilham^a, Tim Niebauer^b, Chris Pearson^c and Peter Molnar^a

^aCIRES and Geological Sciences, University of Colorado, Boulder, CO, USA; ^bMicro-g LaCoste, Inc., Lafayette, CO, USA; ^cSchool of Surveying, University of Otago, Dunedin, New Zealand

ABSTRACT

We quantify changes in gravity that have occurred over the past 15 years at 14 points between latitudes 42.5°S and 44°S in the South Island of New Zealand. Ten of the points form two transects across the Southern Alps and four lie in the epicentral region of the 2010 Canterbury earthquakes. At each location gravity was measured using an absolute gravimeter (FG5–111) with a nominal accuracy of 1 μGal . Observed changes in gravity varied from -53 to $+43$ μGal in the presence of surface elevation changes in the range -11 cm to $+20$ cm. Despite the difficulty in quantifying gravitational contributions from surface and subsurface water, uplift in both the Southern Alps and the Christchurch region is consistent with a Bouguer surface gradient of approximately 1.97 $\mu\text{Gal cm}^{-1}$, appropriate for the mean density of crustal rocks.

ARTICLE HISTORY

Received 24 July 2015
Accepted 4 October 2015

KEYWORDS

Earthquake deformation;
Gravity New Zealand;
mountain growth; water
mass balance

Introduction

The central South Island of New Zealand (Figure 1) currently deforms in response to oblique continental convergence between the Pacific and Australian plates at a rate that has been steady since ≈ 20 Ma (Cande & Stock 2004). The present-day and 3 Ma average relative plate velocities are each ≈ 39 mm a^{-1} , with a shortening component normal to the Alpine Fault of 6 – 9 mm a^{-1} (Beavan et al. 2002; DeMets et al. 2010) and with uplift of control points at rates of up to 5 mm a^{-1} (Beavan et al. 2010a).

In February 2000 and January 2015 we co-located six measurements of absolute gravity and GPS in the Southern Alps (Figure 1), and measured an additional six through Arthur's Pass that were not co-located but are nonetheless surrounded by a cluster of GPS points. The GPS measurements indicate components of vertical velocity of up to 5 mm a^{-1} with measurement uncertainties of ≈ 0.3 mm a^{-1} . The vertical rates show a generally consistent pattern, with low values on the west coast growing to a maximum of ≈ 5 mm a^{-1} near the highest topography and decreasing to low values near Mt John (Beavan et al. 2010a).

The experiment was conceived to examine the rate of decrease of gravity associated with the rate of rise of rock points in the mountains in order to distinguish between several hypothesised mechanisms for mountain growth, and the balance between erosion and uplift. The experiment has met with limited success however, because of the difficulty in quantifying changes of gravity resulting from unmodelled subsurface water level changes.

Absolute gravity

The FG5 gravimeter (Figure 2) was selected for the measurements since under laboratory conditions it can attain 1 μGal long-term repeatability (Niebauer et al. 1995). The acceleration due to gravity on a rising rock surface is expected to decrease because of its increased distance from the centre of the Earth (-3.086 $\mu\text{Gal cm}^{-1}$), but since the increased radial distance includes a layer of rock with finite density, the appropriate gradient for points on the Earth's surface is less. The resulting Bouguer gradient depends on the density of the rising rock. For a crustal layer with average density 2.67 g cm^{-3} , the Bouguer gradient is -1.967 $\mu\text{Gal cm}^{-1}$. For rock with density 3.3 g cm^{-3} , as would be the case if the entire Earth's crust rose at the speed that the surface rises, it is -1.703 $\mu\text{Gal cm}^{-1}$. These calculations assume an infinite sheet of rock with the indicated density. In 15 years, the elapsed time between our two measurements (February 2000–January 2015), we therefore anticipated a maximum increase in height of 7.5 cm and an associated maximum reduction of gravity of 15 μGal in those points rising most rapidly, an effective measurement accuracy of $\approx 6\%$. We discuss the various environmental factors that reduce this accuracy in the following.

The FG5 gravimeter measures the acceleration (m s^{-2}) of a freely falling mass in a vacuum using two atomic standards: a Rubidium atomic clock to measure time; and a stabilised laser to measure distance. Since both standards are invariant (there is no drift) it is in principle possible to repeat the measurement after any interval of time to obtain a comparison between old

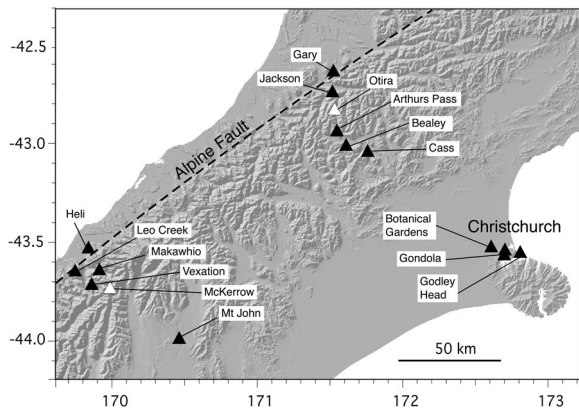


Figure 1. Location of absolute gravity points measured in 2001 and 2015. White triangles were not recovered in 2015.

and new values. The FG5–111 instrument was identical in both measurement years with one exception: the Iodine laser in 2000 was replaced in 2015 with a ML-1 polarisation stabilised laser. The ML-1 laser is less temperamental than the Iodine laser in a non-laboratory environment. However, it uses two frequencies on each side of a stable centre point (Niebauer et al.

1988), requiring an average value from a pair of measurements (typically separated by a 15-minute interval) for the centre value to be obtained. The two frequencies lie precisely on each side of the reference frequency under constant temperature and pressure conditions (which modulate the laser cavity length), but should a significant change in either occur between the two measurements the average value might deviate from the centre frequency value. Measurement accuracy may be reduced to $5 \mu\text{Gal}$ under worst-case environmental conditions, and hence a long series of values is needed to approach an accuracy of $1 \mu\text{Gal}$. In some locations it was possible to gather data with a duration of several days, but in mountain locations measurements were limited to no more than about 5 hours.

A gravity measurement consists of dropping a free-falling cube-corner in a vacuum and, from its observed position as a function of time, calculating its acceleration. Each measurement takes less than 1 s to derive a value and uncertainty for g . The acceleration due to gravity is slightly less at the start of its descent than at its end, and the calculation includes this second-



Figure 2. FG5 absolute gravimeter set up at Leo Creek prior to erecting the instrument tent. The higher cylinder is the evacuated dropping chamber, and the lower cylinder houses a spring-mounted inertial mass to isolate the instrument from microseisms. The electronic control module is housed in the large box behind the gravimeter. The dome and antenna mount of the Leo Creek GPS point is visible extreme right. Water level fluctuations in a small lake below and 100 m north of the point may be responsible for unmodelled gravity changes between 2000 and 2015.

order term. Since the free-fall length is finite and its height above the point depends on the set-point of levelling screws, the measurement is always referred to an arbitrary but precisely specified comparison height, typically 1 m above the measurement point. For this reason the local free-air gradient in gravity above the point must be known. This is measured independently using a relative gravimeter between the point and a platform 1.5 m above the point. From the single measurement and its assumed random measurement error, an average value with reduced uncertainty is derived by repeating the measurement numerous times. Typically, a set of measurements has a duration of 30 minutes and consists of 100 measurements acquired at intervals of 8 s on each of the two frequencies of the ML-1 laser. The measurement uncertainty of each set is therefore the average of the standard deviations of the two frequencies, each reduced by the square root of 100. Outliers above a user-specified threshold are excluded from the averaging. To estimate the integrity of numerous other time-varying corrections (tides, atmospheric pressure, temperature, etc.) several sets of data are recorded over a period of hours and, where possible, several days. The average of all the observed sets, weighted by their measurement uncertainties, provides a time-averaged measure of gravity at the point and its standard deviation.

The procedure adopted in New Zealand was typically to assemble and align the instrument over the survey mark (Figure 3) and wait for the laser to stabilise (1–2 hours). A set of measurements was obtained for 15 minutes on each of the ML-1 frequencies and repeated every hour. On mountain ridges where the instrument was deployed by helicopter and operated in a tent, measurements were undertaken continuously (pairs of sets every 30 minutes) for up to 7 hours, yielding an average value determined from 14 sets of data. The 7-hour window was dictated by helicopter daylight access including set-up and dismantling times of 2–3 hours. In less challenging locations, data with a duration of several days could be obtained yielding an average value based on more than 100 sets of data.

The raw data and a narrative description of each site can be found in Datasets S1–S15. Summaries of adopted values are listed in Table 1.

In practice, the measurement of absolute gravity is subject to numerous sources of noise: tides, changes of mass in the atmosphere, changes of subsurface water distribution and changes of mass and its distribution in glaciers. Corrections for some of these can be made precisely through measurement or calculation, and some can be verified by inspection. For example, numerical corrections for ocean-loading tides, body tides and atmospheric pressure variations can be

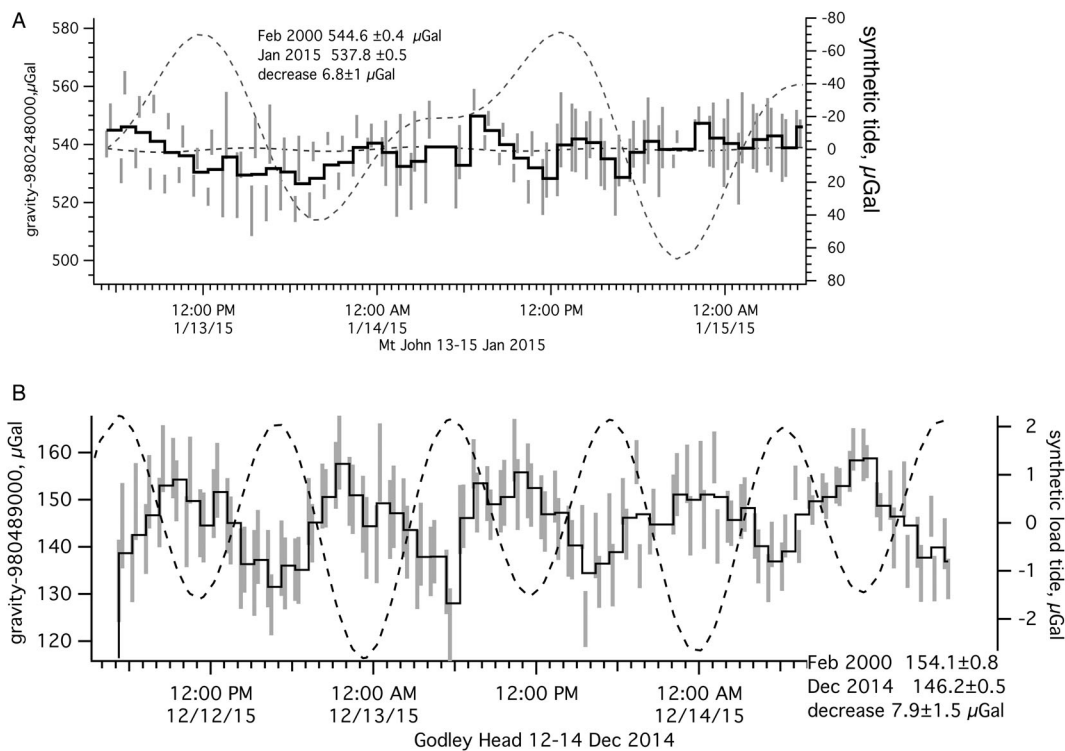


Figure 3. **A**, Thirty-six hours of processed data from Mt John obtained from the FG5–111 using an ML-1 laser. Vertical lines indicate standard deviation for contiguous 15 minute ‘blue’ or ‘red’ datasets corrected for tides and atmospheric pressure. The continuous cityscape line indicates the moving average for each pair. The dashed lines indicate the large body and minor load tide corrections that were applied to the data. **B**, Fifty-five hours of data from Godley Head showing a residual tide ($\approx 20 \mu\text{Gal}$) following ineffective application of the predicted load tide (dashed line $\pm 5 \mu\text{Gal}$). This is the only site where the ocean tide was poorly predicted. The special sensitivity to ocean levels here is due to its high elevation on a promontory surrounded by sea, and it suggests that unknown ocean surge levels may also have perturbed earlier observations at this site.

Table 1. Observed absolute gravity, February 2000 and January 2015. The measured values are all for 1.000 m above the point, and uncertainties are given \pm μ Gal. The negative free-air gradient (Grad) was measured at each site in 2000 but not in 2015. The most significant five digits only are indicated for the 2015 data. An operational narrative, a file of observation parameter, and a numerical listing of datasets for each location are provided in Datasets S1–S15.

Location	Latitude (°S)	Longitude (°E)	Grad μ Gal/cm	Elevation (m)	Feb2000 μ Gal	\pm	2015 μ Gal	\pm	μ Gal/cm	Error
Godley Head ¹	–43.588	172.804	3.60	125	980489152.4	2.0	9141.3	2.0	–7.5 ^a	3
Gondola Low	–43.588	172.716	2.95	50	980505179.9	0.9	5121.4	0.8	–43.4	1.5
Gondola Top	–43.589	172.717	3.81	445	980421716.2	1.4	1672.7	1.5	–43.5	3
Botanical Gdns	–43.53	172.62	3.60	6	980493985.3	5.1	4038.4	2.4	+53.1	7.5
Cass	–43.035	171.759	3.05	589	980272118.5	0.5	2100.3	0.3	–19	1.5
Bealey Hotel	–43.02	171.61	2.73	631	980261187.8	0.3	1179.3	0.4	–8.6	1
Arthur's Pass	–42.95	171.57	2.33	772	980229009.9	1.2	8990.7	0.5	–8.6	1.5
Gary's Rock	–42.649	171.54	4.41	120	980359858.8	1.0	9814.8	1	–40.4	2.5
Otira	–42.832	171.56	2.11	501	980291981.4	0.3	destroyed			
Jacksons	–42.747	171.51	2.79	250	980336050.9	1.0	6044.0	1.5	–6.9	1.5
Makawhio	–43.72	169.85	4.86	1630	980091624.6	0.6	1634.2	1.3	+9.8	2
Vexation	–43.637	169.893	4.4	1475	980131601.1	1.0	1588.3	0.9	–12.8	2
McKerrow	–43.73	169.98	4.4	2150	980038648.7	0.4	under ice			
Leo Creek	–43.643	169.737	5.15	1630	980188398.4	0.5	379.1	0.7	–19.3	2
Mount John	–43.987	170.465	3.91	1600	980248544.6	0.4	8537.8	0.5	–6.8	1
Helipad	–43.534	169.841	2.92	44	980439547.4	2.0	9547.8	1.3	+0.4	2.5

^aThree measurements of gravity are available before and after the earthquake from Godley Head (See Figure 4 and Table 3).

visually verified after application by their absence in time series with durations of several days (Figure 3). The least tractable of these corrections concerns the mobility of inland surface and subsurface water.

With a measurement span of fewer than 5 hours, it is not possible to undertake a visual inspection the credibility of the data; this would not be needed in a normal laboratory environment, where environmental conditions are constant and the microseismic noise level is typically low. Noise levels in New Zealand were significantly higher than in our calibration base in Colorado, presumably because of nearby surf and background seismicity. Numerous earthquakes including one M_w 6 event occurred between December 2014 and January 2015. An example of how the formal accuracy of the measurements can be misleading is to consider a 5-hour moving average of the data shown in Figure 3A. The deviation of contiguous 5-hour segments from the ensemble average exceeds 5 μ Gal.

The effect of subsurface water depends on the porosity of the underlying rock. A porous sand with a fluctuating water table can affect the gravity measurement by up to 1 μ Gal per 25 mm of water level change. In weakly fractured granite, the effect can be as little as 1 μ Gal per 10 m change in water level. At no locations were subsurface measurements of water table available either in 2000 or in 2015. This proved to be a limiting factor that impedes our interpretation of the gravity data in terms of purely deep-seated processes.

At one Alpine point (Lame-Duck/Makawhio) a slight increase in gravity was detected, despite uplift of the point indicated by GPS. We attribute this to ice melt maintaining the water table artificially high on the ridge where the point was located. In 2000 the site was dry with no remaining snow or standing water on the ridge. In January 2015 several snow drifts were present, and one directly next to the point was found to be slowly melting. The resulting trickle of water flowed directly down the

hill, overflowing vertical fissures in rock, suggesting that a transient and significantly large water mass lay on and within the ridge at the time of the 2015 measurement.

Gravity at Gary's Rock NW of Arthur's Pass had decreased by an unexpectedly large amount (40 μ Gal). No direct measure of uplift exists here but interpolated GPS elevation changes suggest no more than 3 cm of uplift had occurred, which would account for a maximum 6 μ Gal of this decrease. We provisionally attributed the remaining 34 μ Gal to the equivalent of an 86 cm thick water layer draining from within the surrounding swamp. The explanation is plausible since, according to local people, the region has been artificially drained of water starting two decades previously. Casting doubt on this explanation, however, we noted that surface stream levels appeared no different from the time of the first measurements in 2000.

Instrument operation

Altogether the field system weighed roughly 200 kg with generator, tent and packing materials. The packages were slung in a net below a helicopter between sites in the mountains, and transported in a minivan between sites accessible by road. The instrument typically took one person 90 minutes or more to assemble, and an hour to disassemble and pack. More lengthy assembly times were usually associated with levelling the two coaxial air-gap-separated tripods on uneven ground and erecting a tent over the instrument. At remote sites the instrument was operated from a 1 kW generator buffered by an uninterruptible power supply, arranged to permit the refuelling of the generator every few hours. Moist air entered the super-spring at one Alpine location, which froze overnight and required the spring-spring assembly to be heated externally using the exhaust gas from the generator before early morning operation could commence.

Table 2. Gravity change (μGal) and change predicted from the Bouguer gradient ($-1.967 \mu\text{Gal cm}^{-1}$) and the known or inferred elevation change of the measurement point. Excess μGal indicates the observed deviation from this predicted value, also expressed as a water-equivalent infinite layer in the penultimate column.

Site	Obs (μGal)	Δ cm	Bouguer (μGal)	Excess (μGal)	Depth water (cm)	Notes
Godley Head ^a	-7.5	2	-5.9	-1.6	-4.0	Coseismic+ocean+landslide
Gondola Low	-43.4	20	-59.3	15.9	40.5	Coseismic Littleton datum
Gondola Top	-43.5	19	-56.4	12.9	32.7	Coseismic Littleton datum
Botanical Gdns	51.5	-11.2	33.2	18.3	46.4	Coseismic (high water table)
Cass	-19	3.3	-9.8	-9.2	-23.4	
Bealey Hotel	-8.6	3.9	-11.6	3.0	7.5	Inferred uplift rate
Arthur's Pass	-8.6	3.9	-11.6	3.0	7.5	Inferred uplift rate
Jacksons	-6.9	3.6	-10.7	3.8	9.6	Inferred uplift rate
Gary's Rock	-40.4	3	-8.9	-31.5	-80.0	Swamp drained
Makawhio	9.8	8.6	-25.5	35.3	89.7	Snowdrift melting
Vexation	-12.8	5.4	-16.0	3.2	8.2	Dry flat lake bed to north
McKerrow		7.2	-21.4			Not occupied
Leo Creek	-19.3	2.85	-8.5	-10.8	-27.5	Leo lake level?
Mount John	-6.8	4.5	-13.4	6.6	16.6	Lake Tekapo level?
Helipad	0.4	1.5	-4.5	4.9	12.3	Uncertain water table

^aSee Table 3 and Figure 4.

The FG5-111 performed well during the measurements after correcting for a number of minor problems following international air transport: vibration during transit had caused loosening of boards and plugs, a superspring damping magnet had become detached and required repair and a loose wire in the 4 kW ion-pump high-voltage supply initially caused an intermittent loss of vacuum. The impaired vacuum remained undetected initially because the ion-pump sensor, linked directly to the high-voltage source, indicated no malfunction. The automatic barometer record occasionally malfunctioned, but in this event pressures were recorded manually. Slow warm-up of the laser at two sub-zero-temperature (degrees Celcius) points required the construction of an insulating jacket around the laser housing.

Results

Datasets S1-S15 provide site descriptions and experimental measurement details at each site. Numerical results are summarised in Tables 1-3. The Christchurch epicentral data are summarised in Figures 4 and 5 and the Alpine transect data are summarised graphically in Figures 6 and 7.

Gravity changes associated with the Canterbury 2010-2011 earthquake sequence

Four points whose elevations were shifted by the Canterbury earthquake sequence that commenced in 2010 were measured in 2000. The sequence, which is still ongoing, started with the M_w 7.0 Darfield earthquake to the west (Beavan et al. 2010b) and continued with

Table 3. Gravity at Godley Head 1995-2015. The instantaneous value is 980,489,000 μGal plus the value indicated in column 3. Due to unmodelled load tides and episodic ocean surges that result in variable loading and gravitational attraction, the observed values show considerable more variance than the formal uncertainties. Adopted values in bold are plotted in Figure 5. A coseismic decrease of 7.0-11.2 μGal occurs in 2010 (see Figure 5).

Source	Epoch	μGal	Sets	$\pm \mu\text{Gal}$
Sasagawa (1996)	15-19 Oct 1995	157.7		2.2
Bilham et al. (2000) ¹	5-6 Feb 2000	146.8	37	3.5
Start fringe 24	5 Feb 2000	151.3	7	2.8
Bad super-spring	6 Feb 2000	145.8	25	1.8
Load tide unsuppressed	23-27 Feb 2000	153.6	197	1.8
All the Feb 2000 data ^a	5-27 Feb 2000	152.4	234	1.6
Start fringe 35 (reported)	5 Feb 2000	154.1	7	0.5
Rogister et al. (2009) ^b	2-4 Dec 2009	151.2		2.4
Rogister et al. (2011) ^b	5-7 Nov 2011	143.2	31	2.4
Observed Dec 2014	12-14 Dec 2014	146.0	132	0.5
Observed Jan 2015	24-25 January	137.7	44	0.4
Observed average 2014/5	Dec 2014-Jan 2015	142.6	178	0.5
Stagpoole et al. (2015) ^c	28 January 2015	144.2	24	3

^aThe mean value for Godley Head in February 2000 based on 55 hours of data ($152.4 \pm 1.6 \mu\text{Gal}$) is less than the reported value ($154.1 \pm 0.5 \mu\text{Gal}$) based on the first 7 hours. The 154.1 μGal reported value was obtained by delaying the GH020500.ddt 5 February 2000 starting fringe to 35 (from 24) and rejecting all the data 6 February onwards. The adopted value indicated on line two was based on a subset of the first seven sets, ignoring the 227 sets obtained at this site later in February 2000. A 'bad' superspring was responsible for high noise in the 6 February data (25 sets) with its average value $145.8 \pm 1.9 \mu\text{Gal}$. However, superspring noise was also absent in the 25/26 February subset with its value of $149.8 \pm 1.2 \mu\text{Gal}$, and it is possible that a lower value than that adopted in the 2000 gravity report is reasonable given the $\approx 20 \mu\text{Gal}$ residual tide noted here (the 7 hours recorded on 5 February 2000 samples only a fraction of this unmodelled local tide). The low uncertainty (0.5 μGal) assigned to the 5 February 2000 data is also considered too optimistic, and should be increased to at least $\pm 2 \mu\text{Gal}$. The 5-27 February average is therefore probably more realistic and we adopt $152.4 \pm 2 \mu\text{Gal}$ as the most probable value.

^bObtained with gravimeter FG5-206 and with an applied free-air gradient of $-3.6 \mu\text{Gal cm}^{-1}$.

^cObtained using gravimeter FG5-237 with a measured free-air gradient of $-3.51 \mu\text{Gal cm}^{-1}$ (Stagpoole et al. 2015), 3 days after our last measurement of the point with gravimeter FG5-111 which used our February 2000 gradient of $3.60 \mu\text{Gal cm}^{-1}$.

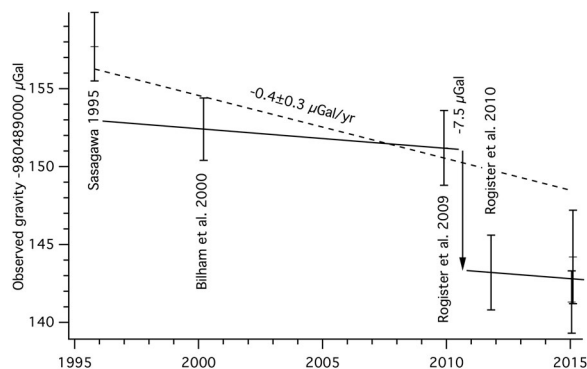


Figure 4. Gravity apparently declined at Godley Head in the 15 years prior to the 2010 earthquake (arrow) if we consider a measurement in 1995, but by an insignificant amount if this first point is neglected. The coseismic offset ($7.5 \pm 3 \mu\text{Gal}$) is little changed whether this slope is considered or not.

a sequence of damaging earthquakes that have progressed to the east (Sibson et al. 2011; Beavan et al. 2012). We do not consider the nature of faulting in these earthquakes. Instead we focus on 2010–2015 height changes measured by Land Information New Zealand (LINZ).

The Botanical Garden site is the former workshop of a 1901–1969 magnetic observatory, the concrete floor of which hosts Christchurch-A, a gravity reference base station for South Island, New Zealand. A nearby benchmark (LINZ AF30) sank 11.2 cm between our 2000 and 2015 measurements, and gravity at the point was found to have increased by $53.1 \mu\text{Gal}$. The site lies in the footwall of a blind, oblique thrust fault with strike 58° and dip 68° SSE with a maximum slip of 2 m (Beavan et al. 2012). Boreholes show that 9 m of gravel overlies a sequence of liquefiable silt and sand layers to 21 m depth. Wother-spoone et al. (2014) make a case for liquefaction having

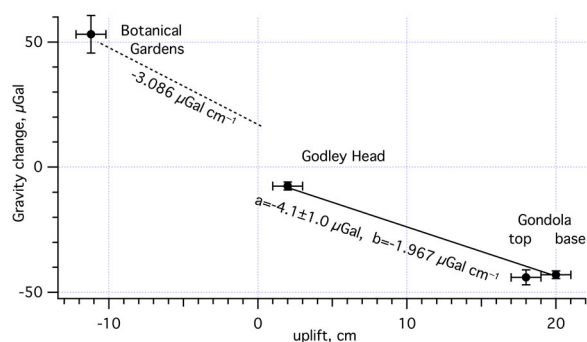


Figure 5. Coseismic gravity and elevation changes near Christchurch. For positive gravity change the slope of the free-air gradient is shown: for gravity decrease a least-squares fit to the data is shown with intercept, a and slope b . The changes at Godley Head are uncertain due to coseismic landslides and unmodelled oceanic effects near the measurement point. The increase in gravity at the Botanical Gardens location is larger than expected from subsidence in the presence of a free-air gravity gradient (dashed); this would be appropriate if all elevation change occurred by compaction of sediment below the site, but is consistent with an increase in the water table level by 45 cm.

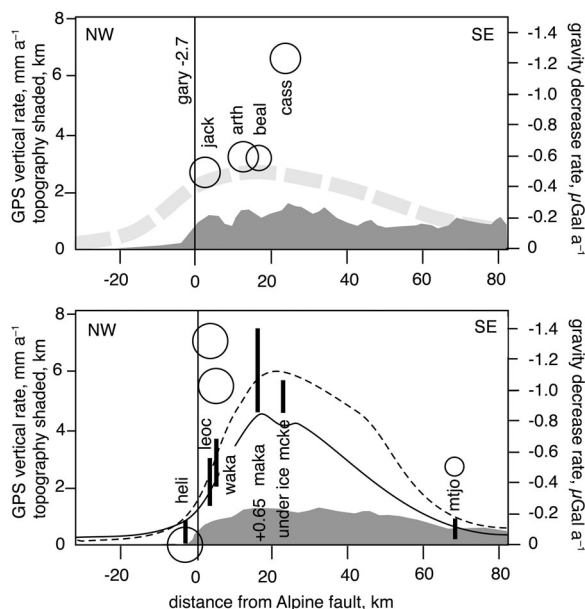


Figure 6. GPS uplift rates (bars with uncertainties from Beavan et al. 2010a) and observed gravity decrease rates (circles sizes proportional to uncertainty) as a function of distance from the Alpine fault. Two gravity outliers are not plotted (see text). Since no GPS points are co-located with the gravity points at Arthur's Pass, the grey thick dashed curve, which is a cubic spline fit to nearby GPS data (Beavan et al. 2010a), is used to estimate uplift rates and cumulative uplift during 2000–2015.

occurred in the deeper layers during the M_w 6.3 22 February 2011 Christchurch earthquake based on an interpretation of strong motion data, but sand was not vented at the surface through the shallow gravel layer. Possible compaction occurred with or without mass loss. The observed subsidence therefore represents a combination of surface lowering, mass loss and tectonic deformation.

In February 2000, calibration points were placed at the base and top of the Mt Cavendish gondola

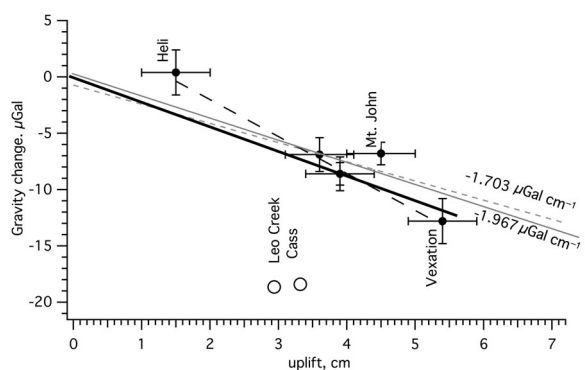


Figure 7. Height changes v. gravity changes for the Alpine Fault traverses. Excluding two outliers, a least-squares fit through the origin yields a gravity gradient of $2.15 \pm 0.14 \mu\text{Gal cm}^{-1}$ (bold line). The bold dash line is a least-squares fit to the data without the constraint of passing through the origin (gradient $-3.3 \pm 0.8 \mu\text{Gal cm}^{-1}$ with intercept $4.5 \pm 3.3 \mu\text{Gal}$). The named Bouguer gradients depicted are fits to the data using imposed slopes appropriate for the rise of Moho ($-1.703 \mu\text{Gal cm}^{-1}$ grey dashed-line) or crustal ($-1.967 \mu\text{Gal cm}^{-1}$, grey solid line) rock, respectively.

separated by 395 vertical metres to serve as a calibration base for spring-based relative gravimeters in New Zealand. These two points rose ≈ 20 cm in the earthquake and, when remeasured in 2015, gravity at each of these points was found to have decreased by 43.5 μGal .

A point at Godley Head on a 125 m high peninsula surrounded on three sides by sea was measured in 1995 (Sasagawa 1996), 2000 (Bilham et al. 2000), 2009 and 2010 (Rogister et al. 2009), December 2014 and January 2015 (this report) and 28 January 2015 with FG5–235 (Stagpoole et al. 2015). These data are summarised in Table 3. A secular reduction in gravity between 1995 and 2009 of $0.4 \pm 0.2 \mu\text{Gal a}^{-1}$ is evident if we include the 1995 data, and $0.1 \mu\text{Gal a}^{-1}$ if the 1995 data are ignored. The reasons for a secular change of gravity at Godley Head could be related to a long-term decay in the water table within the headland ($10 \pm 5 \text{ mm a}^{-1}$), but it is also possible that it represents an artefact of the measurements. Because the least-squares fits converge close to the date of the earthquake, the 2010 coseismic change in gravity is not greatly affected by the pre-2000 data. We calculate that it is $7.3 \mu\text{Gal}$ if the slope is included and $7.8 \mu\text{Gal}$ if it is neglected (Figure 5). We adopt a value of $7.5 \pm 3 \mu\text{Gal}$ for the coseismic change in Figures 4 and 5.

The formal uncertainty of the 2015 Godley Head measurement ignores two systematic errors that reduce its measurement accuracy. The first error arises from the ocean tides, which are poorly removed by synthetic predictions of the ocean load tide, and the second is related to coseismic mass wasting.

The poor removal of the load tide is evident in the time series from the site in February 2000, November 2011, December 2014 and January 2015 (Figure 3B and Datasets S1–S15), and from the scatter in the observed data (Table 3). The residual tide evident in the data (Figure 3B) has an amplitude of $\approx 20 \mu\text{Gal}$ and is caused by a combination of loading and direct mass attraction of the ocean waters that surround the Godley Head promontory on three sides. The gravitational effects of the ocean are higher here than at any of the other sites we measured because a small change in sea level approximates an infinite layer subtending a narrow angle ($20\text{--}30^\circ$) with the gravity vector. Changes in ocean height subtend a much smaller angle inland and their effects are reduced by the cosine of this angle. Since the load tide is clearly inaccurately modelled, so too are ocean surges whose amplitudes are determined by oceanic currents and prevailing winds.

Errors in tidal prediction can be suppressed by observing continuously for several days and by truncating the averaged series to a multiple of sidereal days, but could be further suppressed by using gravity predictions from the tide gauges located near Christchurch and Littleton. We do not attempt this here due to uncertainties in the potentially large mass wasting that occurred at the

time of the earthquake. Landslides on the edge of the cliff within a few hundred metres of the measurement point increased gravity by transferring mass from the top of the cliff to its base. At their starting location the cliff materials would have attracted the gravimeter almost horizontally and would have contributed little to measured gravity. At their resting point in the surf zone below the site they would increase gravity at the point. A precise calculation of the gravity contribution from the landslides is difficult due to the unknown distributions of mass before and after the earthquake.

Gravity changes across the Southern Alps, 2000–2015

In the two arrays crossing the Southern Alps two sites were not recovered, and the data from an additional two are considered to be contaminated by unknown subsurface changes in the distribution of water mass. Of the two sites not recovered, one site was destroyed near Arthur's Pass (Otira) and the highest point (McKerrow) was still covered in ice in January and was inaccessible. It might be possible to recover the Otira site in the future since its concrete foundation remains, but the removal of many tons of buildings from the site and the presence of a 4 m high pile of rubble near the probable location of the point rendered the value of its re-measurement uncertain in 2015. McKerrow could also be occupied in the future when it is clear from snow and ice.

In our introductory section we dismissed data from two sites that yielded results that were considered inconsistent with their assumed uplift, the point Gary and the point Makawhio. The value for gravity at Gary decreased by $40 \mu\text{Gal}$ due to inferred subsurface water drainage, and the value for gravity at Makawhio increased because of the proximity to surface ice. These values are indicated as numerically offscale in the velocity plot shown in Figure 6. Two additional sites appear to be outliers due to their apparently large increases of gravity (Leo Creek and Cass).

In Figure 7 we plot gravity change v. uplift for the 2000–2015 period. If we assume that a zero change of height is associated with a zero gravity change, the remaining five points appear to be rising within a gravity gradient of $-2.15 \pm 0.13 \mu\text{Gal cm}^{-1}$. Two least-squares slopes are plotted, one with a constrained Bouguer gradient of $-1.703 \mu\text{Gal cm}^{-1}$ appropriate for uplift of dense mantle type densities (3.3 g cm^{-3}) and the other with a constrained gradient of $-1.967 \mu\text{Gal cm}^{-1}$ appropriate for crustal rocks (density 2.65 g cm^{-3}). These least-squares fits with their artificially constrained slopes both intersect the 'zero' uplift axis close to zero.

Discussion

We first clarify a distinction between the measured local free-air gravity gradient, which is site-specific,

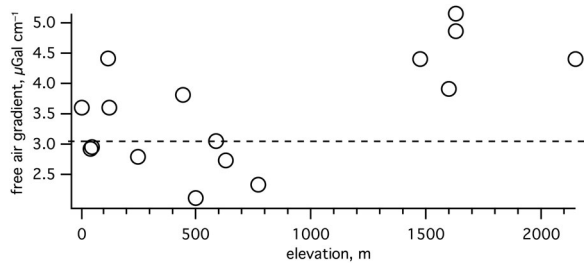


Figure 8. Observed free-air gradients at different elevations compared to the mean free-air gradient at the Earth's surface ($-3.086 \mu\text{Gal cm}^{-1}$, dashed line). Uncertainties are approximately equal to the diameter of each circle.

and a regional free-air gravity gradient, which is not. In February 2000 we measured the free-air gradient at each location between a point flush with the ground and at points 0.5 m and 1.5 m above ground level. The local free-gravity gradient determined with a relative gravity meter from these three readings is needed to reduce the observed gravity data to a comparison elevation precisely 1 m above the measured mark. These measured free-air gradients vary by a factor of more than two (Figure 8).

The local free-air gradient in the few metres above a point is the sum of an inverse-square reduction in gravity attributable to the increasing distance from the Earth's centre of mass, plus a contribution from a terrain correction resulting from the distribution of mass near the site. The first is precisely determined by the elevation, and the second can be considered constant to first order. This is because the contributions to the gravity gradient from local terrain depend on mass distributions and subsurface rock densities below and above the point, whose contributions decay inversely with the cube of their distance. Their contributions are further diminished by the cosine of their angle to the vertical gravity vector; mass variations near the area beneath the point therefore exert the largest influence. With the exception of the Godley Head landslide, the rock terrain near each site changed insignificantly between 2000 and 2015; its contribution can therefore be considered invariant. However, a varying mass of ice a few metres from the point, or a heterogeneous distribution of subsurface water beneath the point, has both a direct influence on the observed gravity and a minor perturbation to the observed gradient. Ideally the free-air gradient would have been measured at each epoch to verify this time invariance, but in our case this was undertaken only at Godley Head (in 1995, 2000 and 2009) where the gradient was measured four times (Sasagawa 1996; Bilham et al. 2000; Rogister et al. 2011; Stagpoole et al. 2015) and at Mt John where the gradient was measured twice. Local free-air gravity gradients are effectively 'fixed' to the point and move with it. In summary, a gravimeter monitoring at a fixed elevation above the point encounters little or no change from the local free-air gradient whether or not

a vertical tectonic translation of the point occurs. In a rising mountain region, gravity is decreased in proportion to a rate governed by a regional gravity gradient determined by deep-seated processes beneath the region, or by local mass transfer into or from the region.

Interpretation of gravity v. uplift data

The graph of uplift v. gravity reduction across the Southern Alps shown in Figure 7 permits three interpretations. In one, we may assume that the reduction in gravity is proportional to height change, an assumption that requires a least-squares fit to the data to pass through the origin. This first assumption yields a best-fitting slope to the data, with an apparent gravity gradient of $\approx 2.15 \pm 0.14 \mu\text{Gal cm}^{-1}$ (bold solid line).

In the second interpretation we assume that uniformly distributed mass changes are occurring in the region independently of height changes, effectively relaxing the requirement that a least-squares fit must pass through the origin. The weighted least-squares fit to the six points in Figure 7 (the Bealey and Arthur's Pass points are superimposed) has slope $3.3 \pm 0.8 \mu\text{Gal cm}^{-1}$ with a positive intercept of $4.5 \pm 3.3 \mu\text{Gal}$. Since the gradient so derived exceeds the Earth's free-air gradient, the solution may be discarded as implausible. The rejection of this least-squares fit implies that the uncertainties in Heli and Vexation are greater than those we have assigned to these points.

In the third interpretation we impose an appropriate gravity gradient and fit this to the data in a least-squares sense (Figure 7). We proposed two end-member Bouguer gradients in our introductory remarks: one appropriate for the rise of the Moho ($-1.703 \mu\text{Gal cm}^{-1}$; grey dashed line) and one involving a rise of crustal rocks alone ($-1.967 \mu\text{Gal cm}^{-1}$; grey solid line). In Figure 7 we show the best fits of these constrained slopes to the data, and note that half of our data are outliers to these gradients. These slopes do not pass through zero, but this is an unimportant criterion in a region where erosion or glacial mass changes may prevail. It is therefore clear from Figure 7 that our data do not permit us to choose between Bouguer gradients influenced by crustal or mantle uplift, one of the goals of the project. For these subtle slopes to be distinguished it is also readily apparent that measurement accuracies would need to be equal or better than $1 \mu\text{Gal}$ over the extreme ranges of uplift. Such accuracies currently present a challenge in a mountain environment.

We note that if it were possible to assign the correct Bouguer gradient, the least-squares intercept on the 'zero' uplift axis would quantify a flux of mass into, or out of, the region. Significant regional erosion, or the removal of water mass by receding glaciers for example, would have resulted in a negative intercept in Figure 7.

Clearly, these interpretations are simplistic but, in the presence of unknown local contributions from

subsurface water table contributions to the observed gravity, more complex solutions are considered unwarranted.

Future measurements of gravity points to investigate uplift processes

The absence of direct measurements of the subsurface water table levels results in large uncertainties in all the measurements discussed above. At four locations (Cass, Gary, Leo Creek and McKerrow) we consider the observed data sufficiently anomalous to merit exclusion from quantitative interpretation. From [Figure 7](#) we conclude that uncertainties were also underestimated at two other points (Heli and Vexation). We recognise that a weak numerical test for the potential presence of large local mass changes would have been possible had we measured the local gravity gradient at each site in 2015 in addition to measurement of its absolute value. Some sites are clearly less affected by subsurface water than others. In particular, a measurement high above a coastal region (such as Godley Head) should be avoided since uncertainties in sea level map strongly into the local gravity vector. One possibility in future studies would be to locate gravity measurements on islands with low relief in lakes where the local water level may be measured precisely, and where the local mass changes subtend a large angle to the gravity vector.

The dependence on the measurements of hidden changes of water table was anticipated when the experiment was originally conceived, but we hoped that water table changes would not be as severe as they have in practice proved to be. We also hoped that the measurements could be conducted several times (e.g. at 5-year intervals) in order to estimate the time-varying contribution to gravity change from hydrology. The cost of shipping the absolute gravimeter to remote points thwarted these plans. However, the measurements in 2015 suggest a less expensive mode of measurement might be considered using a hybrid measurement process: a precise relative gravimeter deployed at numerous locations to complement the results from a single absolute measurement at an easily accessible site.

Relative gravimeters have a $\approx 1 \mu\text{Gal}$ relative measurement accuracy but have limited vertical measurement range (e.g. $\approx 200 \text{ mGal}$, equivalent to $\approx 650 \text{ m}$). As a result, although they are unable to measure differences in gravity between sea level and 2 km elevations to an accuracy of $1 \mu\text{Gal}$, it would be possible to measure a cluster of points between 1500 m and 2100 m, the range of high-elevation points in the Southern Alps, to this level of relative accuracy tied to a single absolute gravity measurement within this measurement range. The five Alpine points near Fox Glacier could be measured by helicopter traverse in a single day, compared to the 5 days of fine weather

needed with the absolute gravimeter traverse. Similarly, the Arthur's Pass traverse could be undertaken by road in single day. The ease with which relative gravity measurements could be conducted would permit several measurements each year to be made to densify the measurements, to examine seasonal variations and to assess the validity of some of the assumptions in the above discussion.

Conclusions

Fourteen of the sixteen measurements of absolute gravity made in February 2000 were repeated in January 2015 in the South Island of New Zealand, yielding in most locations combined accuracies in measured changes of the order of $2 \mu\text{Gal}$. In addition to the changes of elevation that were under investigation, significant changes in gravity were detected that we attributed to large changes in the distribution of water near some of the sites. An interpretation of a subset of these measurements, where the influence of local effects appears to be small, suggests that subtle regional mass changes can be detected.

In both the Southern Alps and in the epicentral region of the Christchurch earthquakes, a combined free-air and Bouguer gravity gradient of approximately $-1.9 \mu\text{Gal cm}^{-1}$ provides a satisfactory agreement between uplift and the reduction in gravity. A precise determination of the Bouguer gradient at each location was not, however, possible from our data due to uncertainties in the local contributions to gravity from surface and subsurface water. Our results are therefore unable to distinguish between models of uplift of the Southern Alps rising because of deep-seated processes involving dense mantle rocks or shallower processes in the Earth's crust.

The absence of direct knowledge of the depth of water table in both 2000 and 2015 renders the total uncertainty of the measurements much larger than the formal accuracy of the FG5 absolute gravimeter. A possible solution to characterise the noise contribution from local mass changes would be to increase the number of gravity measurements both spatially and temporally using a hybrid approach of a few absolute gravity points at selected elevations, supplemented by relative gravimeter targeted at a limited elevation range. In addition, measurements of gravity at locations where the local water table can be precisely monitored might be considered, such as islands of low relief within large lakes where the water level can be measured directly.

Supplementary data

Dataset S1. Arthur's Pass.

File S1. Arthur's Pass site narrative.

File S2. Arthur's Pass one – Micro-g Solutions processing report.

File S3. Arthur's Pass one – dataset.

File S4. Arthur's Pass two – Micro-g Solutions processing report.

File S5. Arthur's Pass two – dataset.

Dataset S2. Bealey Hotel.

File S6. Bealey Hotel site narrative.

File S7. Bealey one – Micro-g Solutions processing report.

File S8. Bealey one – dataset.

File S9. Bealey two – dataset.

Dataset S3. Botanical Gardens.

File S10. Botanical Gardens site narrative.

File S11. Botanical Gardens one – Micro-g Solutions processing report.

File S12. Botanical Gardens one – dataset.

Dataset S4. Cass.

File S13. Cass (University of Christchurch field station) site narrative.

File S14. Cass one – Micro-g Solutions processing report.

File S15. Cass one – dataset.

File S16. Cass two – Micro-g Solutions processing report.

File S17. Cass two – dataset.

Dataset S5. Gary's Rock.

File S18. Gary's Rock site narrative.

File S19. Gary's Rock one – Micro-g Solutions processing report.

File S20. Gary's Rock one – dataset.

Dataset S6. Godley Head.

File S21. Godley Head site narrative.

File S22. Gravity measurements in South Island New Zealand, Feb. 2000 narrative.

File S23. Gravity measurements in South Island New Zealand, Feb. 2000 – dataset.

File S24. Godley Head one – Micro-g Solutions processing report

File S25. Godley Head one – dataset.

File S26. Godley Head two – Micro-g Solutions processing report

File S27. Godley Head two – dataset.

Dataset S7. Gondola (bottom).

File S28. Gondola (bottom) site narrative.

File S29. Gondola (bottom) – Micro-g Solutions processing report.

File S30. Gondola (bottom) – dataset.

Dataset S8. Gondola (top).

File S31. Gondola (top) site narrative.

File S32. Gondola (top) – Micro-g Solutions processing report.

File S33. Gondola (top) – dataset.

Dataset S9. Helipad.

File S34. Helipad site narrative.

File S35. Helipad one – Micro-g Solutions processing report.

File S36. Helipad one – dataset.

Dataset S10. Jacksons Garage.

File S37. Jacksons Garage site narrative.

File S38. Jacksons Garage – Micro-g Solutions processing report.

File S39. Jacksons Garage – dataset.

Dataset S11. Leo Creek.

File S40. Leo Creek site narrative.

File S41. Leo Creek – Micro-g Solutions processing report.

File S42. Leo Creek – dataset.

Dataset S12. Makawhio.

File S43. Makawhio site narrative

File S44. Makawhio – Micro-g Solutions processing report.

File S45. Makawhio – dataset.

Dataset S13. Otira.

File S46. Otira site narrative.

Dataset S14. Vexation.

File S47. Vexation site narrative.

Dataset S15. Mt John.

File S48. Mt John site narrative.

File S49. Mt John – Micro-g Solutions processing report.

File S50. Mt John – dataset.

Acknowledgements

The measurement of gravity at the GPS points in the Southern Alps was conceived in discussions with John Beavan in 1999, and we have used his 2010 calculations of velocity to extrapolate elevation changes to 2015 levels. Fred Klopping kindly prepared the University of Colorado FG5-111 for deployment in December 2014, and he and Derek van Westrum responded to operational issues as they arose during the 2015 field measurements. Measurements at NOAA's Table Mountain Gravity Observatory before and after the experiment confirmed the repeatability of the FG5-111 to 1.5 μ Gal. We thank Land Information New Zealand for providing us with elevation change data near Christchurch, and the Godley Head trust and the University of Canterbury for permitting access to the Godley Head and the Cass Field Station, respectively. Vaughan Stagpoole kindly provided us with a draft copy of results of the 2015 GNS Absolute-g measurements of Mt John and Godley Head. The Arthur's Pass police kindly permitted us to use their jail for measurements, and the managers of Bealey Hotel and Jacksons Retreat allowed us to measure gravity in their garages. The manuscript was considerably improved by critical reviews from the Associate Editor, F. Caratori Tontini and an anonymous reviewer.

Associate Editor: Dr Pilar Villamor.

Disclosure statement

No potential conflict of interest was reported by the authors.

Funding

We thank NSF for funding the project in 2000 (EAR 9902981) and in 2015 (EAR 1519035 RAPID). Field costs for some of the 2014 measurements were born with support from the Crafoord Foundation.

References

- Beavan J, Motagh M, Fielding EJ, Donnelly N, Collett D. 2012. Fault slip models of the 2010–2011 Canterbury, New Zealand, earthquakes from geodetic data and observations of postseismic ground deformation. *New Zeal J Geol Geophys.* 55:207–221. doi:10.1080/00288306.2012.697472.
- Beavan J, Tregoning P, Bevis M, Kato T, Meertens C. 2002. The motion and rigidity of the Pacific Plate and implications for plate boundary deformation. *J Geophys Res.* 107:2261. doi:10.1029/2001JB000282.
- Beavan RJ, Denys P, Denham M, Hager B, Herring T, Molnar P. 2010a. Distribution of present-day vertical deformation across the Southern Alps, New Zealand, from 10 years of GPS data. *Geophys Res Lett.* 37: L16305. doi:10.1029/2010GL044165.
- Beavan RJ, Samsonov S, Motagh M, Wallace LM, Ellis SM, Palmer NG. 2010b. The Darfield (Canterbury) earthquake: geodetic observations and preliminary source model. *Bull New Zeal Soc Earthq Eng.* 43:228–235.
- Bilham R, Crawford R, Niebauer T. 2000. Gravity measurements in South Island New Zealand, February 2000. Report prepared for Land Information New Zealand. Wellington: LINZ.
- Cande SC, Stock JM. 2004. Pacific–Antarctic–Australia motion and the formation of the Macquarie Plate. *Geophys J Int.* 157:399–414. doi:10.1111/j.1365-246X.2004.02224.x.
- DeMets C, Gordon RG, Argus DF. 2010. Geologically current plate motions. *Geophys J Int.* 181:1–80. doi:10.1111/j.1365-246X.2009.04491.x.
- Niebauer NT, Faller JE, Godwin HM, Hall JL, Barger RL. 1988. Frequency stability measurements on polarization-stabilized He–Ne lasers. *Appl Opt.* 27:1285–1289.
- Niebauer TM, Sasagawa GS, Faller JE, Hilt R, Klopping F. 1995. A new generation of absolute gravimeters. *Metrologia.* 32:159–180.
- Rogister Y, Amos M, Le Moigne N. 2009. Absolute gravity observations at Godley Head, New Zealand, 2–4 December 2009. Report prepared for Land Information New Zealand. Wellington: LINZ.
- Rogister Y, Bernard J-D, Winefield R, Collett D. 2011. Absolute Gravity Observations at Godley Head, New Zealand, 5–7 November 2011. Report prepared for Land Information New Zealand. Wellington: LINZ.
- Sasagawa G. 1996. Absolute Gravity observations at Godley Head, New Zealand. Report prepared for Land Information New Zealand. Wellington: LINZ.
- Sibson RH, Ghisetti FC, Ristau J. 2011. Stress control of an evolving strike-slip fault system during the 2010–2011 Canterbury, New Zealand, earthquake sequence. *Seismol Res Lett.* 82:824–832.
- Stagpoole VM, Dando N, Caratori Tontini F, Black J, Amos N. 2015. Absolute gravity observations at principal New Zealand stations 2015. GNS Science Report, 2015/46. Lower Hutt: GNS Science.
- Wotherspoon L, Orense RP, Green R, Bradley B, Cox B, Wood C. 2014. Analysis of liquefaction characteristics at Christchurch strong motion stations. In: Orense RP, Towhata I, Chouh N editors. *Soil liquefaction during recent large earthquakes*. Boca Raton, FL: CRC Press; p. 33–43.